

Comparison of Results from In-House Solidification Convection Model with Standard Benchmark

R. DYJA*

Częstochowa University of Technology, 42-201 Częstochowa, Poland

Doi: [10.12693/APhysPolA.139.525](https://doi.org/10.12693/APhysPolA.139.525)

*e-mail: robert.dyja@icis.pcz.pl

This paper focuses on a problem of solidification with convection. The performance of a developed model against a standard benchmark of solidification commonly found in literature is presented. The developed model is based on the Navier–Stokes equation and the energy equation with the convection term and also takes into account the latent heat of solidification. This set of equations is numerically solved by the finite element method. In order to overcome numerical difficulties arising from solving the Navier–Stokes equation, the streamline upwind Petrov Galerkin and the pressure stabilized Petrov Galerkin types of the FEM formulation are used. The resulting numerical model is implemented in the C++ programming language with the use of state of the art numerical libraries which allows it to be run on high-performance computers. The comparison of results from the in-house model with results obtained by other authors allows to verify the validity of the chosen methods and implementation. The inclusion of convection in the solidification model allows to extend the model with the possibility of prediction of macrosegregation or cavity occurrence, both of which are important for the prediction of defects in foundry processes.

topics: FEM, solidification, convection, numerical simulation

1. Introduction

Solidification is a difficult problem to prepare a mathematical description of it. From the physical point of view, it involves heat transfer with a phase change and a moving interface that divides two phases (in the case of a pure metal solidification) [1] or a mushy zone that is a mixture of the solid and liquid phases (in the case of alloys solidification) [2].

Heat transfer in solidification problems can be in the form of conductivity and convection. While the conductive heat transfer is usually easy to solve and does not require very computationally intensive techniques, more detailed models have to use computational fluid mechanics for the introduction of convective heat transfer, which comes with a great computational cost [3, 4].

There is a trend of using algorithms prepared for high-performance computing, when dealing with problems involving computational fluid mechanics [5].

Because of this, the solidification problem is still a popular research topic. Researchers use different numerical methods to solve equations arising from the physical model. Very popular are finite differences, finite volumes and finite elements [6].

The major goal in simulations of solidification is to improve the technological processes and the quality of products [7]. In this topic, researchers

can focus on different scale sizes: microscopic or macroscopic. All of them can be important for refining technological parameters. This work focuses mostly on simulations done at the macroscopic scale. The author presents numerical model of solidification and its performance in one of popular benchmark problems involving phase change and liquid phase flow.

2. Mathematical model

The governing equation for modeling the solidification process is based on the energy transfer equation:

$$\rho \frac{\partial H}{\partial t} + \rho (\mathbf{u} \cdot \nabla) H = \lambda \nabla^2 T, \quad (1)$$

where ρ is the density, H is the enthalpy, T is the temperature, \mathbf{u} is the velocity from the convection force, λ is the thermal conductivity and t is the time.

With the use of the apparent heat capacity formulation [8] and assuming that the solid phase velocity in the mushy region is zero, it is possible to express (1) in the following way:

$$c^* \frac{\partial T}{\partial t} + \rho c (\mathbf{u} \cdot \nabla) T = \lambda \nabla^2 T, \quad (2)$$

where c^* is the approximation of the effective heat capacity, which includes the latent heat of solidification.

The boundary condition, used in the model presented with (2), is the Dirichlet boundary condition (boundary condition of the first type) on external sides of casting.

For the approximation of the effective heat capacity, various methods can be used. Some of them may pose numerical difficulties during calculations, but all of them give very similar results [9]. In this work, the Morgan method is used. Hence,

$$c^* = \frac{H^n - H^{n-1}}{T^n - T^{n-1}}, \quad (3)$$

where n in the upper script is the time level.

Liquid metal in this model is assumed to be a Newtonian fluid. This allows to write the Navier–Stokes set of equations as:

$$\rho \left(\frac{d\mathbf{u}}{dt} + (\mathbf{u}\nabla)\mathbf{u} \right) + \rho\mu \left((\nabla\mathbf{u}) + (\nabla\mathbf{u})^T \right) - \nabla p + \rho\mu \frac{f_1}{K_\varepsilon} \mathbf{u} = \rho f \quad (4)$$

and

$$\nabla \cdot \mathbf{u} = 0, \quad (5)$$

where p is the pressure and μ is the viscosity.

The last term of the left-hand side part of (4) is, in general, a drag force. This term describes the flow of liquid metal in a porous medium that appears in the mushy zone. Here, f_1 is the liquid fraction and K_ε is the permeability of the mushy zone. A drag force appears in the mushy zone from the interaction between liquid and already solidified metal, and severely slows down the velocity of liquid metal in the mushy zone.

In the presented model, it is assumed that the solid phase is immovable [10]. The permeability of the mushy zone is approximated by the Kozeny–Carman equation:

$$K_\varepsilon = K_0 \frac{f_1^3}{(1 - f_1)^2}, \quad (6)$$

where K_0 is the secondary dendrite arm spacing.

The right-hand side part of (4) describes body forces that arose in the liquid. This part is connected with the buoyance force that is approximated by the Boussinesq formula:

$$f = -g\beta(T - T_0), \quad (7)$$

where β is the expansion coefficient, g is the gravitational acceleration, T_0 is the reference temperature, which in this case was the temperature from initial conditions.

The liquid fraction and the solid fraction are connected with a simple relation, i.e.,

$$f_l = 1 - f_s, \quad (8)$$

where the value of f_s is taken from the phase equilibrium graph relationship

$$f_s = \frac{1}{(1 - k)} \frac{T_L - T}{T_M - T_L}, \quad (9)$$

where T_L is the liquidus temperature, T_M is the solidification temperature of the pure component and k is the solute partition coefficient.

Now, an appropriate set of initial and boundary conditions should be attached to (4). An initial value of \mathbf{u} is set as for the initial condition, while the no-slip condition is used on walls of the casting domain in order to force the velocity value to be zero on those boundaries. Then, (4) and (5) are solved numerically with the help of the stabilized finite element method. Details concerning the application of this method can be found in [11].

3. Problem setup and simulations results

The data for the benchmark problem was taken from [12]. It consists of the solidification problem inside a closed cavity. A schematic picture of the region with the added description of boundary conditions can be seen in Fig. 1. The computational area is a regular square with a side length equal to 0.05 m.

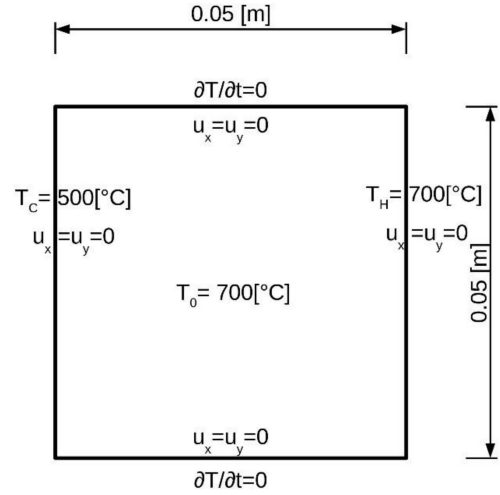


Fig. 1. Computational domain used for benchmark problem.

TABLE I

Thermophysical properties of alloy under study, together with boundary and initial temperatures.

Property	Value
conductivity	100 W/(m °C)
specific heat	1000 J/(kg °C)
density	2500 kg/m ³
latent heat	400000 J/kg
viscosity	0.0025 kg/(m s)
coefficient of thermal expansion	4.0 × 10 ⁻⁵
solidus temperature	550 °C
liquidus temperature	650 °C
melting point of pure aluminium	675 °C
partition coefficient	0.14
cold side temperature	500 °C
hot side temperature	700 °C
initial temperature	700 °C

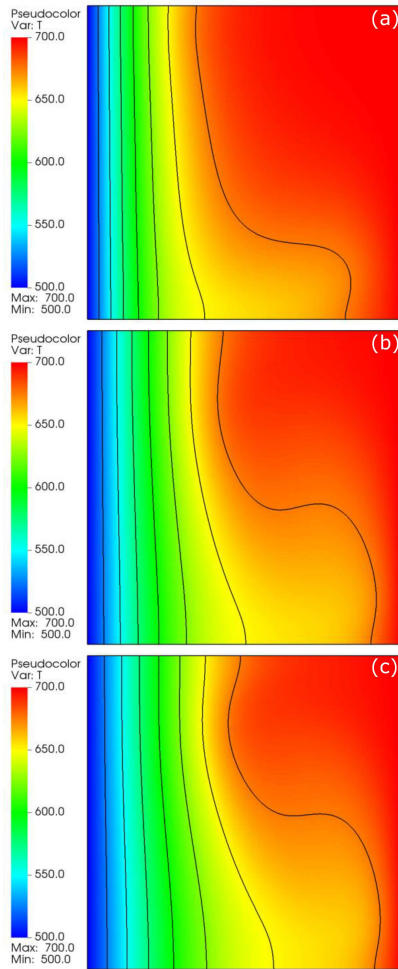


Fig. 2. Temperature distributions: (a) after 5 s, (b) after 10 s and (c) after 15 s.

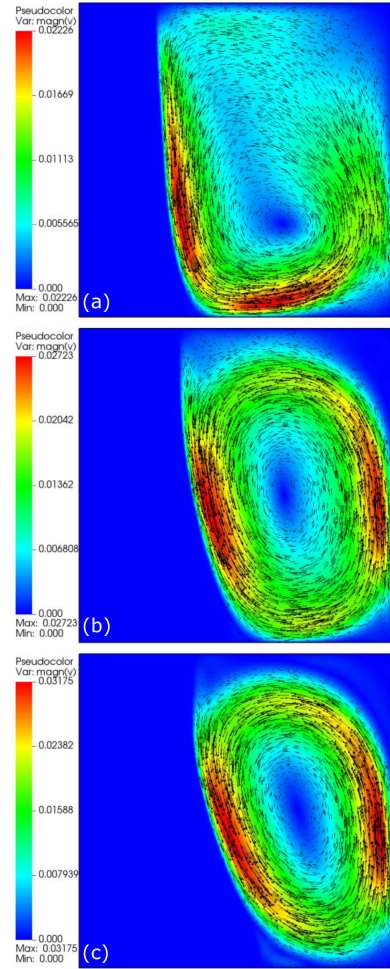


Fig. 3. Velocity profiles: (a) after 5 s, (b) after 10 s and (c) after 15 s.

It is assumed that the whole area is filled with a molten alloy. Physical details of this alloy are listed in Table I. It has physical properties close to the Al_4Cu alloy. It is assumed that in the initial state the molten alloy is in the uniform temperature of $700^\circ C$, just above its liquidus temperature. Boundary conditions for this problems are: the top and bottom sides have perfect insulation, while the left side of the area cooled to temperature $500^\circ C$. The right side has the presumed temperature of $700^\circ C$. For the left and right sides, the Dirichlet boundary condition was used. The top and bottom sides use the Neumann boundary condition with zero flux.

Figures 2 and 3 present the results of simulation with the author's model. The figures present the profiles taken at moments of 5, 10 and 15 s of the simulation time. The results were obtained from the model based on solving (4) and (5) with the stabilized finite element method. Besides physical properties presented in Table I, the following numerical parameters were used: the size of the time step equal to 0.05 s and the average size of the triangle finite element equal to 2.0×10^{-4} m.

Temperature profiles in Fig. 2 show that the convection as isothermal lines do not form vertical lines. Instead, the hot liquid metal is pushed by the buoyancy force close to the top of the cavity and solidification occurs mostly at the bottom of the cavity. Velocity vectors in Fig. 3 show that the movement of the liquid phase in this problem is anti-clockwise. Both of those behaviors are expected and were reported by other authors who conducted simulations for this benchmark [12, 13].

4. Conclusions

Based on temperature profiles, it can be seen that a qualitative behavior of the presented model is correct. It can be observed that the layer of the solidified metal is thicker at the bottom of the region. Based on the velocity plot, it can be observed that velocity vectors of the liquid metal have anti-clockwise orientation. This behavior is in agreement with physical observations. Moreover, the obtained temperature profiles are also in good agreement with temperature profiles presented by other authors.

References

- [1] T. Skrzypczak, *Arch. Metall. Mater.* **57**, 1189 (2012).
- [2] C.R. Swaminathan, V.R. Voller, *Metall. Mater. Trans. B* **23**, 651 (1992).
- [3] J.C. Heinrich, D.R. Poirier, *C.R. Mécanique* **332**, 429 (2004).
- [4] M. Salcudean, Z. Abdullah, *Int. J. Numer. Methods Eng.* **25**, 445 (1988).
- [5] T. Garcia, P. Spiteri, G. Khemliche, *Adv. Eng. Softw.* **131**, 116 (2019).
- [6] B. Mochnecki, J. Suchy, *Numerical Methods in Computations of Foundry Processes*, Polish Foundrymen's Technical Association, Kraków 1995.
- [7] V.R. Voller, C.R. Swaminathan, B.G. Thomas, *Int. J. Numer. Methods Eng.* **30**, 875 (1990).
- [8] T. Skrzypczak, L. Sowa, E. Węgrzyn-Skrzypczak, *Archiv. Foundry Eng.* **20**, 37 (2020).
- [9] R. Dyja, E. Gawronska, A. Grosser, P. Jeruszka, N. Sczygiol, in: *Transactions on Engineering Technologies*, Eds. S.-I. Ao, H.K. Kim, M.A. Amouzegar, Singapore 2015, p. 1.
- [10] W.D. Bennon, F.P. Incropera, *Int. J. Heat Mass Transf.* **30**, 2161 (1987).
- [11] S. Deep, N. Zabararas, *Int. J. Numer. Methods Eng.* **64**, 1769 (2005).
- [12] C.R. Swaminathan, V.R. Voller, *Int. J. Numer. Methods Heat Fluid Flow* **3**, 233 (1993).
- [13] I. Ik-Tae, K. Woo-Seung, L. Kwan-Soo, *Int. J. Heat Mass Transf.* **44**, 1507 (2001).